Pergamon

Adv. Space Res. Vol. 18, No. 6, pp. (6)221–(6)230, 1996

0273–1177/96 $9.50 + 0.00

0273–1177(95)00928–0

MODEL OF THE MID-LATITUDE IONOSPHERIC TROUGH ON THE BASE OF COSMOS-900 AND INTERCOSMOS-19 SATELLITES DATA

A. T. Karpachev,* M. G. Deminov* and V. V. Afonin**

* *IZMIRAN, 142092 Troitsk, Moscow Region, Russia*
** *Institute of Space Research, Moscow, Russia*

ABSTRACT

A new model of the mid-latitude ionospheric trough is developed on the base of Intercosmos-19 and Cosmos-900 satellites data (over 1500 orbits). It is valid for the nighttime (18 to 06 MLT), winter and equinox, K_p-indices from 0 to 8. It covers the topside ionosphere up to 1000 km and describes the trough minimum position Λ_T depending on longitude λ, altitude h, local magnetic time MLT and K_p-index. Model is presented in the analytical form, as well as a nomogram versus MLT and K_p and a nighttime segment of a circle (in the polar coordinate system) with the radius depending on the K_p-index. The effective K_p-index taken for preceding 4.4 hours is used in the model. Agreement between the model and other data on the trough and the equatorial boundary of the auroral oval is discussed.

INTRODUCTION

Variations of the position of the minimum of the mid-latitude (or main) ionospheric trough (MIT) in the various models are usually expressed by a linear dependence on local time t and K_p -index as: $\Lambda_T = \Lambda_o - \alpha K_p - \beta t \pm 2^o$, where t = 0 corresponds to midnight and K_p is the actual value of the magnetic activity index. The accuracy of these models is not better than 2^o since, due to a number of causes, the data scatter is very large: by errors in the data themselves, inadequacy of the linear relationship and by dependence on the longitude, season, other indices (D_{st}, AE or B_z) and so on. Many attempts have been made to find a more effective relationship between Λ_T and K_p or some another magnetic activity index. Correlations with AE, D_{st} or B_z were found to be weaker than with K_p /1/, and the introduction of a 3h time delay decreased the correlation coefficient from 0.65 down to 0.61 /2/. Some models admit a more precise non-linear relationship between Λ_T and local time /3,4/ but the data scatter was not significantly diminished. Largely different values were found for the coefficient in the relations: at midnight Λ_o varies from 60^o /5/ to 65.5^o /3/, α from 0.7 /6/ to 2.1 /7/, β from 0.23 /6/ to 0.75 /8/. The correlation coefficient r did not exceed 0.6 to 0.7. The present paper is an attempt to improve the accuracy of the Λ_T model by taking into account the Λ_T variations with the longitude and altitude; introducing more effective $K_p^*(\tau)$-index (τ being proportional to $\Delta K_p/\Delta t$); more careful data processing.

MODEL DESCRIPTION

The model is based on in-situ measurements of local plasma density from Cosmos-900 satellite (more than 1200 passes) and on sounding data from Intercosmos-19 satellite (about 300 passes), during solar maximum ($F_{10.7} \approx 200$) in 1978-1980, mostly in local winter and partly in equinoxes. Data cover both hemispheres in the longitude interval $\lambda = 0 - 360^o$, magnetic local time MLT = 18–06 h and magnetic activity $K_p = 0 - 8$. Intercosmos-19 data refer to heights of the F2-layer maximum. Cosmos-900 had almost circular orbit, its height decreased from $\simeq$ 500 km to $\simeq$ 350 km during the life time. The measurements were repeated with a period 0.64 s so that the trough minimum could easily be determined with accuracy better than 0.5^o.

The model is expressed in eight equations describing variations of the invariant latitude of the trough minimum position Λ_T with the longitude λ, altitude h, magnetic local time t and K_p-index:

$$\Lambda_T(h, \lambda, t, K_p^*) = \Lambda_o - \Delta\Lambda_T(K_p^*) - \Delta\Lambda_T(t) - \Delta\Lambda_T(h, \lambda, K_p^*) \quad (1)$$

$$\Delta\Lambda_T(K_p^*) = \alpha(t)K_p^* \quad (2)$$

$$\Delta\Lambda_T(t) = \beta(K_p^*)t \quad (3)$$

$$\Delta\Lambda_T(h, \lambda, K_p^*) = A\Delta\Lambda_T(\lambda) + 2[1 + A\Delta\Lambda_T(\lambda)]\Delta\Lambda_T(h) \quad (4)$$

$$A = 1 - 0.1K_p^* \quad (5)$$

$$\Delta\Lambda_T(h) = \exp[(h_m - h)/H] \quad (6)$$

$$\Delta\Lambda_T^N(\lambda) = 0.5[\mathrm{Cos}(2\lambda - 45) - \mathrm{Cos}(\lambda + 40)] \quad (7)$$

$$\Delta\Lambda_T^S(\lambda) = \mathrm{Cos}(\lambda + 35) \quad (8)$$

where $h \geq h_m \approx 350$ km, $H = 200$ km , symbols N and S refer to the Northern and Southern hemisphere respectively, t is taken in hours, h - in km, λ - in degrees; K_p^* is K_p-index averaged over preceding 4.4 h. The equations (2) and (3) are linear relationships between local time t, K_p-index and Λ_T, where coefficient α in equation (2) depends on local time and β in equation (3) on K_p^*. The non-linear relationship between Λ_T and t is shown in Figure 6. The amplitude of the longitudinal variations Λ_T decreases as K_p and altitude increase, (5) and (6). The longitudinal variations of Λ_T are presented by the first harmonic of the Fourier expansion in the Southern hemisphere (8) and by two harmonics in the Northern one (7). Coefficients Λ_o, α and β are shown in Table for two versions; in the first (first column) the linear approximation was performed for the whole MLT interval (18 to 06 h). But since the relationship between Λ_T and t is in fact non-linear, this approximation introduces large errors, especially at the ends of the interval, so the accuracy (standard deviation) σ of the Λ_T estimate for this approximation is not better than 1.9° (last line in the Table). A second version (2nd and 4nd columns) in which the linear approximation is distinct for 18-24 and 00-06 MLT reaches practically the same accuracy as the non-linear approximation ($\sigma \simeq 1.7°$). The local time t = 0 in (1) and (3) corresponds to MLT = 00 in the first version and to MLT = 21 and 03 in the second version. The third column in Table (labelled 00) refers to the most accurate non-linear approximation.

TABLE. Standard deviation and coefficients in equations (1) to (3).

	18-06	18-00	00	00-06
Λ_o	66.3	68.3	65.4	64.5
α	2.35	2.45	2.30	2.25
β	0.55	0.90	-	0.20
σ	1.9	1.7	1.6	1.7

Our description is valid in the whole topside ionosphere from h_mF2 to $\approx$ 1000 km, it is independent of magnetic activity and longitude. Though established for 18-06 MLT, its accuracy decreases near the ends of this interval, especially, in the linear approximation. The model is valid for winter and equinox, although small seasonal variations were revealed in the Cosmos-900 data /12/. Because no dependence of the trough position on solar activity has revealed, the model may be used for any solar activity.

LONGITUDINAL VARIATIONS OF THE TROUGH POSITION

Longitudinal changes of the trough minimum position were first deduced from Ariel-3 satellite data /9/. Stronger variations (up to 10 – 11°) were found in Intercosmos-19 sounding data /10/. Figure 1 shows the longitudinal variations of the trough position in both hemispheres

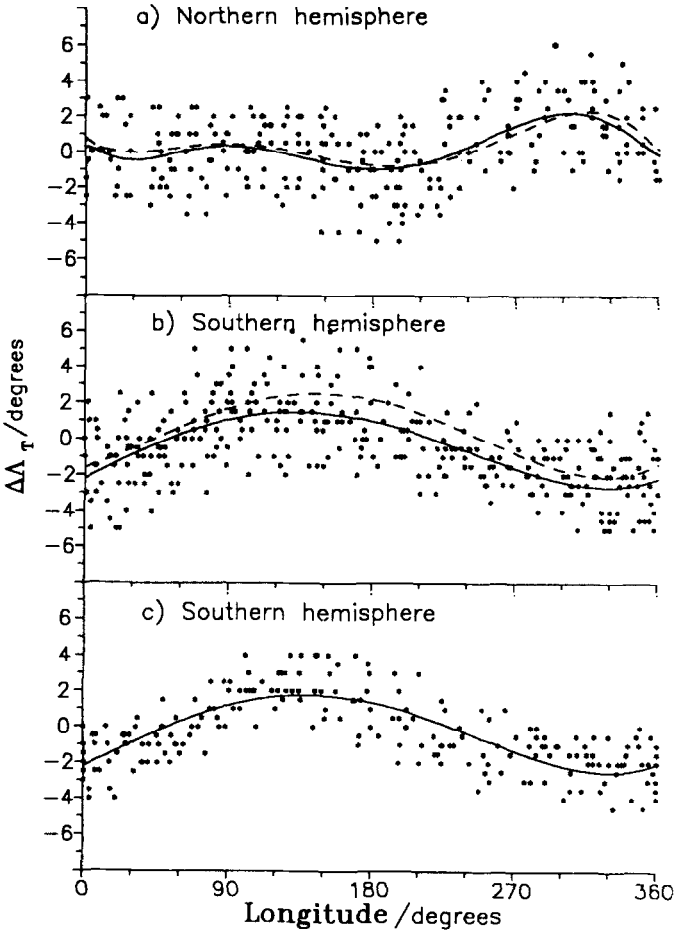

Fig.1. Variations of the trough ninimum position Λ_T with longitude during local winter in the Northern (a) and Southern (b) hemispheres presented as deviations of Cosmos-900 data from model /7/. The approximation is given by the solid lines for winter and dashed lines for equinox. Figure 1c shows the same data as 1b, however without the zero term of the Fouirier expansion.

/11/. The data are presented as deviations of the trough position obtained from the Cosmos-900 satellite data from a model that uses the linear dependence Λ_T on LT and K_p /7/:

$$\Lambda_T = 65.2 - 2.1K_p - 0.5t \pm 2^\circ, \quad (9)$$

where K_p refers to the three preceding hours. Cosmos-900 data refer to winter nighttime (18-06 MLT) quiet ($K_p \leq 3$) conditions at the altitudes 350-500 km. A preliminary analysis of these data has shown that the character of the longitudinal effect weakly depends on local time, at least for midnight hours. It was supposed also that the character of the longitudinal effect does not depend on K_p. With this assumption and equation (9) without the scatter term $\pm 2^\circ$, $\Delta\Lambda_T$ describes purely the longitudinal variations of the trough minimum position, so Λ_T can be written as: $\Lambda_T(\lambda) = \Lambda_o + \Delta\Lambda_T(\lambda)$. Note that for midnight, $\Delta\Lambda_T = 0$ in Figure 1 corresponds to $\Lambda_o \simeq 61^\circ$, since the average K_p is 2 in this data set. The approximation obtained by means of the least-squares method is plotted in Figure 1 by solid lines. For comparison, the approximation for the equinox /12/ is shown by dashed lines too. It appears that the amplitude and the character of the longitudinal effect vary with the season only slightly. In winter the average trough (over all the longitudes) is found a bit nearer to the equator than in equinox. During disturbed conditions the situation is opposite: the winter trough is found to be on the average by 1° more poleward than in equinox. Since all these variations are within error ranges, seasonal variations are neglected in the following.

Figure 1 shows a data scatter is up to 6 – 8°, so that the standard deviation σ is $\simeq$ 1.8°

for both seasons and hemispheres. It is slightly less than the typical standard deviation 2° obtained by processing the trough data (see e.g. /7/). This is explained by taking into account the longitudinal effect and by more careful data processing. In particular, the second trough (more equatorward than MIT) appreciably affecting the statistical pattern was revealed /13/ and excluded from the data set. The data scatter arises from the reasons which are poorly understood yet. But it can yet be decreased by analyzing the longitudinal variations. This may be demonstrated for the Southern hemisphere where we have a maximum of data (335 cases). We selected only those appearing in long sequences and at all longitudes, removing the zero term in the Fourier expansion. The result is shown in Figure 1c. Comparison Figures 1b and 1c shows considerably decreased scatter ($\sigma \simeq 1.3°$), and a correlation coefficient $r \simeq 0.77$ (in the Northern hemisphere r $\simeq$ 0.65). Thus, the longitudinal effect is the regular characteristic of the nighttime subauroral ionosphere both for winter and equinoxes.

Figure 1 also shows that the character of the longitudinal effect is different in both hemispheres. This may be due to the different magnetic field configurations in both hemispheres, in particular the displacement between the geomagnetic and geographic poles /10/.

With good accuracy, the longitudinal variations can be described by the first harmonic of the Fourier expansion in the Southern hemisphere and by two harmonics in the Northern hemisphere:

$$\Delta\Lambda_T^N(\lambda) = -0.2 + 1.2\mathrm{Cos}(\lambda + 40) - 1.1\mathrm{Cos}(2\lambda - 39) \quad (10)$$

$$\Delta\Lambda_T^S(\lambda) = -1.1 - 2.1\mathrm{Cos}(\lambda + 36) \quad (11)$$

It was supposed above that the character of the longitudinal effect do not depend on K_p-index. To test this assumption, the data of the Cosmos-900 for disturbed periods (mean value of $\overline{K}_p = 4$) in the Southern hemisphere were statistically processed and the regression equation has been derived which can be expressed similarly to (11) by the first harmonic of the Fourier expansion:

$$\Delta\Lambda_T^S(\lambda, K_p = 4) = -2.4 - 1.6\ \mathrm{Cos}(\lambda + 28) \quad (12)$$

If to compare (11) and (12) it can be seen the character of the longitudinal effect do not change and its amplitude decreases as K_p-index increases.

ALTITUDE DEPENDENCE OF THE TROUGH POSITION

Let us consider now the dependence of the trough minimum position on altitude. In Figure 2 the longitudinal variations of Λ_T in the Northern and Southern hemispheres obtained from the Cosmos-900 and Intercosmos-19 data (solid and dashed lines respectively) are shown. The Intercosmos-19 data can be expressed similarly to equations (10) and (11) in the form:

$$\Delta\Lambda_T^N(\lambda) = -2.6 + 1.9\ \mathrm{Cos}(\lambda + 26) - 1.4\ \mathrm{Cos}(2\lambda - 59) \quad (13)$$

$$\Delta\Lambda_T^S(\lambda) = -2.6 - 3.3\ \mathrm{Cos}(\lambda + 44) \quad (14)$$

The Intercosmos-19 data were obtained for the same conditions (MLT = 00, $\overline{K}_p = 2$) as the Cosmos-900 data, but for the heights of the F2-layer maximum. The mean value of h_mF2 is $\approx$ 350 km for the midnight hours in the trough region. Satellite Cosmos-900 measured the local plasma density at altitudes $\approx$ 450 km in the Northern hemisphere and $\approx$ 400 km in the Southern hemisphere, i.e. higher than the F2-layer maximum. Note that the $\Delta\Lambda_T$ in Figure 2 is deviation from the model /7/ which was derived from the ESRO-4 satellite data obtained at altitudes 245 – 1177 km, i.e. at $\sim$ 700 km on the average. Comparison of equations (10,11) and (13,14) revealed that: (1) the character of the longitudinal effect is changed only slightly as the altitude increases; (2) its amplitude is decreased by a factor $\simeq$ 1.5 as altitude changes from $\sim$ 350 km to $\sim$ (400 – 450) km; (3) its mean (averaged over

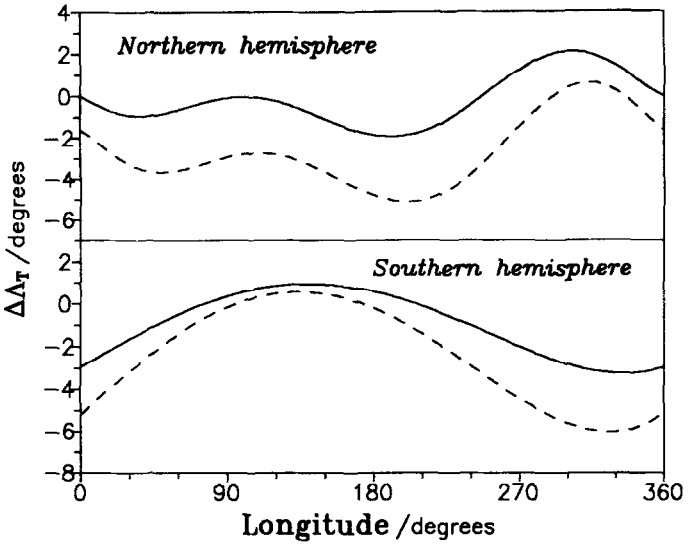

Fig.2. Longitudinal variations of the trough minimum position Λ_T are shown as deviations from the model /7/ of Cosmos-900 data (solid lines) and of Intercosmos-19 data (dased lines) obtained in the Northern and Southern hemispheres for quiet conditions ($\overline{K}_p = 2$).

all the longitudes) position is shifted poleward as the altitude increases. The changes of the trough minimum position are reasonably described by an exponential dependence on the altitude as in equation (6). Thus, the importance of the longitudinal influence decreases as altitude and K_p-index increase, and the trough, on the average, is displaced poleward as altitude grows (see the equation (4)). It is easily to verify from the expressions (4 to 8) that the amplitude of the longitudinal effect is maximum at the heights of the F2-layer maximum peaking with 5 to 6° during very quiet periods. During the strong disturbances ($K_p \geq 6$), the longitudinal effect is weak and can be neglected.

Above approximately 1000 km, the trough position does not practically depend on the altitude: $\Lambda_T = 65.4 - 2.30\ K_p - (1 - 0.1K_p)\Delta\Lambda_T(\lambda)$ for the midnight (non-linear approximation). A rather weak longitudinal effect at these altitudes is associated probably with longitudinal variations of the position of the equatorial boundary of the auroral diffuse precipitation forming the poleward wall of the trough /14/.

The relationship between Λ_T and K_p-index is different at different longitudes. This difference is maximum near the F2-peak. For example, in the Southern hemisphere at midnight, $\Lambda_T = \Lambda_o - 3 - 2.0K_p$ at longitudes near 320°, where $\Delta\Lambda_T(\lambda) \approx +1$, and $\Lambda_T = \Lambda_o + 3 - 2.6K_p$ at longitudes near 140° , where $\Delta\Lambda_T(\lambda) \approx -1$. Similarly, at low magnetic activity at longitudes where $\Delta\Lambda_T(\lambda) \approx +1$, the variations of Λ_T with the altitude are minimum and at longitudes where $\Delta\Lambda_T(\lambda) \approx -1$, they reach 4° as altitude decreases from 1000 km to h_mF2. During periods of high magnetic activity the difference $\Lambda_T(1000) - \Lambda_T(h_mF2)$ is about 2° independently on longitude.

DEPENDENCE OF THE TROUGH POSITION ON THE K_p-INDEX

Taking longitudinal variations into account the dependence of the trough position on the K_p- index may be determined more accurately. Cosmos-900 data were used for equinoxes and local winter conditions in both hemispheres. The three phases of intense disturbances ($K_p \geq 4$): growth phase, main phase maximum and recovery phase, were analysed separately, as well as prolonged (≥ 24 hours) quiet ($K_p \leq 2$) periods. In a first approach the actual K_p value was used and all data were transferred to midnight according to expression (9). Figure 3 shows examples for the storm growth phase (crosses) and recovery phase (squares). A 2nd degree polynomial was chosen as best fit for both phases. The correlation coefficient r is 0.79 for the growth phase and 0.72 for the recovery phase. Standard deviations are 2.5 and 2.2° respectively. Figure 3 shows regressions lines (dashed) for the storm main phase

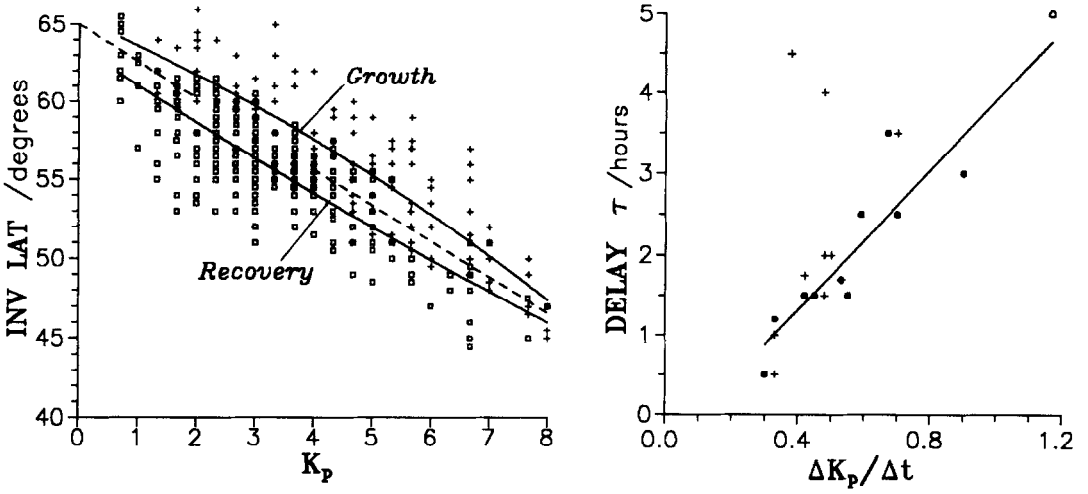

Fig.3. Trough minimum position Λ_T versus K_p during the growth phase (crosses) and recovery phase (squares) of the intense storms recorded aboard Cosmos-900. Non-linear approximations are shown by solid lines. For comparison, the regression lines for the main phase maximum of the storms ($K_p \geq 4$) and prolonged quiet periods ($K_p \leq 2$) are shown by dashed lines.

Fig.4. Dependence of the time delay τ of the trough response to K_p variations on the change rate $\Delta K_p/\Delta t$ for the midnight and morning hours obtained from Cosmos-900 satellite data with the relevant regression line. For comparison, Cosmos-900 data for the evening hours (crosses) and Ariel-3 satellite data for 05 LT taken from /14/ (one open circle) are presented too.

maximum and for prolonged quiet periods too. The correlation coefficient is nearly 0.75 for the both last cases. Linear regression equations are almost identical for all conditions. With the full data set we find: $\Lambda_T = 65.0° - 2.3K_p$, not too different from equation (9). The difference between non-linear approximations for the growth and recovery phases is, however, significant, up to 3.5° . As shows Figure 3, the trough may appear at high latitudes at the growth phase, even for K_p between 4 and 6. Minimum latitude of the trough is reached at the beginning of the recovery phase during which it is sometimes observed at latitudes of 51 – 52° for K_p = 2-3, i.e. by 5 – 6° lower than it evident from equation (9). This is not the main ionospheric trough /13/. All this leads to a strong discrepancy of approximation curves in Figure 3.

The main cause of the discrepancy seems to be a time lag in the trough response to K_p at all phases of a storm. To test this assumption, over 30 intense disturbances ($K_p > 4$) were analysed carefully for the period of 1977-1979 where Cosmos-900 data were available /13/. The analysis showed that the time delay τ of the trough response to the K_p-index variations depends on the K_p-index change rate $\Delta K_p/\Delta t$. This relation appears most clearly in the midnight and morning hours. Therefore ten most representative storms were selected to study the relation between the delay time τ and storm growth rate $\Delta K_p/\Delta t$ for midnight and morning hours. The regression line for this condition is shown in Figure 4 as:

$$\tau = 4.3 - 0.4\Delta K_p/\Delta t, \qquad (15)$$

with a correlation coefficient $r = 0.78$. For comparison, one extreme point is also shown, obtained from Ariel-3 satellite data for a severe storm /15/ . A few cases of extreme delay appear in evening data of Cosmos-900, probably associated with the "polarization jet" /13/

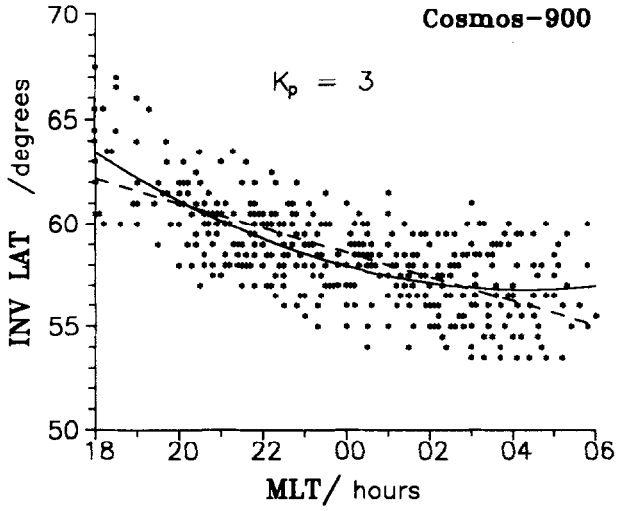

Fig.5. The dependence of the trough minimum position Λ_T obtained from Cosmos-900 data for K_p = 3 on local time. The linear and non-linear approximations are shown.

which could be observed on the storm growth phase during afternoon and evening hours.

Note that for the average change rate $\Delta K_p/\Delta t \approx 0.6$, the delay is of order $\tau \approx 2.2$ h. This explains in part the large data scatter in Figure 3 in which the actual K_p-index was taken. The best correlation will in the average be observed when taking the averaged K_p value for the preceding 4.4 hours.

DEPENDENCE OF THE TROUGH POSITION ON LOCAL TIME AND K_p

Taking into account the longitudinal variations of Λ_T and also the time delay in the trough response to K_p-index changes allows to define more exactly the relationship between Λ_T and local time (and K_p-index too). For this purpose, the Cosmos-900 data for both seasons and both hemispheres were used. All the data (over 1200 cases) were separated into five K_p intervals: 0-1, 1-2, 2-4, 4-6 and 6-8. Since it is rather difficult to deduce a non-linear relationship between Λ_T and local time and K_p-index simultaneously, a linear dependence on K_p was first assumed: $\Delta\Lambda_T(K_p) = 2.3K_p^*(\tau)$ under relatively stable K_p^*-index. The data were transferred to the mean K_p^* value for each interval whereafter mean values and standard deviations of Λ_T were determined. For example, data corrected in this way for $K_p^*= 3$ are presented in Figure 5 with linear and non-linear approximations. Standard deviation σ is $\simeq 1.8°$ for the linear approximation and $\simeq 1.6°$ for the non-linear approximation. After this, the averaged values of Λ_T were corrected by means of interpolation and extrapolation over the whole interval of K_p (0 to 8) and MLT (18 to 06) in linear approximation on K_p and non-linear approximation on MLT. The final result of this procedure is shown in the form of a nomogram versus MLT and K_p in Figure 6. Figure 6 shows that: (1) the trough is shifted rapidly toward the equator in the dusk sector, reaches a minimum position near 4.5 MLT in the morning and then moves slowly back toward the pole; (2) the trough dependence on K_p is strongest in the evening, so that the coefficient attached to K_p in (2) α is $\simeq 2.6$ at 18 MLT, 2.3 at 00 MLT and 2.2 at 4.5 MLT; (3) coefficient β attached to t in (3) in the first linear version depends on K_p^* and changes from 0.7 at $K_p^*= 0$ to 0.5 at $K_p^* = 8$. From Figures 5 and 6, it is also seen that the discrepancy between linear and non-linear approximations is not large (1° for the interval 19-05 MLT), so, it follows that the linear approximation is justified at least during midnight hours. This holds the more for the second version of the linear approximation in which the difference between linear and non-linear approximations is not more than 0.3° in the entire considered local time interval.

The non-linear approximation is expressed in more complicated analytical form (e.g. /3/). It is known however that the position of the equatorial boundary of the diffuse auroral precipitation (EBDP) can be mapped quite well onto a circle (in a polar coordinate system)

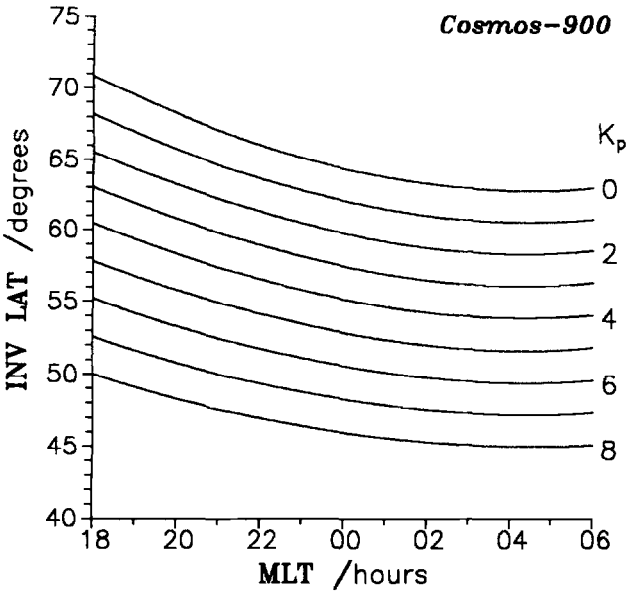

Fig.6. Statistical dependence of the trough minimum position Λ_T on local time and K_p obtained from Cosmos-900 satellite data at altitudes 350-500 km.

with the centre displaced to the aftermidnight hours /16/. Let us present the Cosmos-900 data in the similar form: as a nighttime segment of the circle. In Figure 7, the EBDP position given by the model /16/ according to the DMSP satellites data for $K_p = 0$ and 5 is depicted by the dashed lines. For $K_p = 0$, the circle radius r = 21.1° , and its centre is displaced to 87.6° along the ≈ 2.5 MLT meridian. The Cosmos-900 data (obtained at altitudes of 350-500 km) are shown by dots (for each hour). The best fit is the circle with radius r = 24.2° and centre located at the latitude 86.5° and the meridian 4.0 MLT. It is seen that the discrepancy between the best fit line and the Cosmos-900 data is not more than ±1° reaching +2° only at 18-19 MLT. But at this local time the EBDP true position is located by 1 – 2° more poleward too, since, in fact, the best fit line is not a circle but an ellipse with a small excentricity. The difference between EBDP and the trough minimum positions is, on the average, ≈ 3°, increasing from ≈ 2° at 18 MLT to 4-5° at dawn since the centres of the circles do not coincide. Such a superposition of these structures at different local times is a well known fact (see e.g. /17/).

Comparing to other data sources for $K_p = 0$ we found the trough position closest to the pole in AE-C data (obtained at altitudes of ~ 300 km) /3/, while the most equatorward ones were reported in ground-based sounding data /8/. At 00 MLT, the difference between the EBDP and trough minimum positions is 1.2° in the first case, 5.5° in the second case and 2.5° from the Cosmos-900 data. Thus, the most reasonable agreement between both boundaries seems to exist for the Cosmos-900 midnight data.

Let us consider the dynamics of both structures as K_p increases. For $K_p = 5$ radius of the circle for the EBDP increases to 29.1° and its centre is displaced equatorward (from 87.6° to 85.8°) along the same ~ 2.5 MLT meridian. The trough minimum position is shifted equatorward more significantly than EBDP as K_p increases, so its radius reaches 34.7° for $K_p = 5$. Its centre is displaced from 86.5° to 86.2° and from 4.0 MLT to ~ 3.2 MLT. So the trough and EBDP are shifted to the equator with different rates, the trough displacement being stronger in the evening and the EBDP one in the morning. For $K_p = 5$ the difference between them at different local times may reach 5.5° . It should be pointed out that in another EBDP model built up on the base of Oreol-3 satellite data /18/, for $K_p = 5$, the distance between EBDP and trough minimum is equal to ≈2°, what is usually observed in experiment. This seems to be associated with the fact that in model /16/ actual K_p values were used, whereas in model /18/ K_p -indices were taken over preceding 4.5° hours.

The centre of the best fit circle for the trough is only sligthly depend on K_p changes. There-

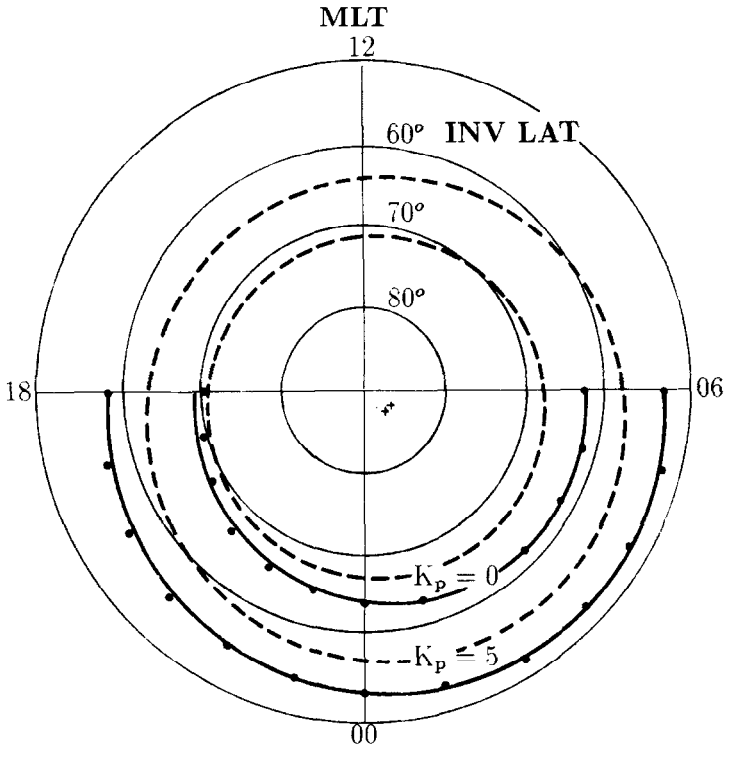

Fig.7. The trough minimum position Λ_T, obtained from Cosmos-900 satellite data for $K_p = 0$ and $K_p = 5$ (dots). Solid lines: best fit (displaced) circles (their centers shown as crosses). For comparison the best fit circles for the equatorial boundary of the diffuse auroral precipitation /16/ are shown too by dashed lines.

fore for the whole interval of K_p (0 to 8) a fixed centre at 86.5° latitude and 3.5 MLT meridian can be adopted leading to $r = 24.0 - 2.3K_p$. The total mean root-square error for this version of the model adds up to $\simeq 1.9°$.

CONCLUSION

Based on Intercosmos-19 and Cosmos-900 satellites data, a more adequate model for the main ionospheric trough has been developed. It is the first to take into account variations of the trough minimum position with longitude and altitude. A new, more effective, index $K_p^*(\tau)$ is introduced where τ depends on the rate of change of K_p and averages over ≈ 4.4 hours. In the most accurate, non-linear approximation the mean-square error σ is $\simeq 1.6°$. In the linear approximation taken for the interval of MLT = 18 – 06h, $\sigma \simeq 1.9°$. The position of trough minimum may be also approximated by the midnight segment of a circle (in the polar coordinate system) centred at 86.5° latitude and 3.5 MLT meridian and with radius $r = 24.0 + 2.3K_p \pm 1.9°$. But the radical reduction of the data scatter has not been gained. It is nessesary to derive a more effective, than K_p-index, magnetic activity index which will be more adequate to represent variation of the trough position. Such an attempt is undertaken in /19/.

Acnowledgements. The autors are grateful to the referees and K. Rawer especially for a very detailed and thorough review of this paper. This work was in part supported by the Russian Foundation for Fundamental Research under grant 94-05-17352.

REFERENCES

1. M.J.Rycroft and S.J.Burnel, Statistical analysis of movements of the ionospheric trough and plasmapause, *J.Geophys.Res.*, 75, #28, 5600-5604 (1970).

2. P.N.Collis and I.Haggstrom, Plasma convection and auroral precipitation processes associated with the main ionospheric trough at high latitudes, *J.Atmos.Terr.Phys.*, 50, #3/4, 389-404 (1988).

3. R.F.Spiro, R.A.Heelis and W.B.Hanson, Ion convection and the formation of the mid-latitude F-region ionisation trough, *J.Geophys. Res.*, 83, #9, 4255-4264 (1978).

4. N.P.Ben'kova, G.A.Jerebtzov, B.G.Dolgoarshinnih et al., Dynamics of the ionospheric disturbances at the high latitudes during the high solar activity period, in: ***The wave propogation in the ionosphere***, (in Russian), Moscow 1986, p.145-154.

5. M.J.Rycroft and J.O.Thomas, The magnetospheric plasmapause and the electron density trough at the Alouette 1 orbit, *Planet.Space Sci.*, 18, #1, 65-80 (1970).

6. A.Best and C.-U.Wagner, Morphology and characteristic parameters of the trough, in: ***The physical processes in the main ionospheric trough region,*** Proceeding of KAPG, Prague 1983, p.19-41.

7. W.Kohnlein and W.J.Raitt, Position of the mid-latitude trough in the topside ionosphere as deduced from ESRO 4 observations, *Planet.Space Sci.*, 25, #5/6, 600-602 (1977).

8. N.P.Ben'kova and E.K.Zikrach, The main ionospheric trough from the ground-based observations in Yakutya, in: ***The physical processes in the main ionospheric trough region,*** (in Russian), Proceeding of KAPG, Prague 1983, p.7-18.

9. Y.Tulunay, Global electron density distributions from the Ariel-3 satellite at mid-latitudes during quiet magnetic periods, *J.Atmos.Terr. Phys.*,35, #2, 233-254 (1973).

10.M.G.Deminov and A.T.Karpachev, Longitudinal effect in the main ionospheric trough.I. The trough position, ***Geomagnetism and aeronomy,***, 26, #1, 63-68 (1986).

11.V.V.Afonin, M.G.Deminov, A.T.Karpachev et al., Longitudinal variations of the main ionospheric trough position for the nighttime winter conditions from Cosmos-900 and Intercosmos-19 satellites data, ***Geomagnetism and aeronomy,*** 32, #2, 75-78 (1992).

12.A.T.Karpachev, V.V.Afonin and Ya.Smilauer, Variations of the midnight trough minimum position with longitude in winter and equinox: a comparison, ***Geomagnetism and aeronomy,*** 34, #1, 70-75 (1994).

13.M.G.Deminov, A.T.Karpachev, V.V.Afonin et al., Dynamics of the mid-latitude ionospheric trough during the storms.I. A qualitative pattern, ***Geomagnetism and aeronomy,*** 34, #1, in print (1995).

14.C.-I.Meng, Diurnal variations of the auroral oval size, *J.Geophys.Res.*, 84, #9, 5319-5324 (1979).

15.K.Tulunay and A.R.W.Hughes, A satellite study of the mid-latitude trough in electron density and VLF radio emissions during the magnetic storm 25-27 May 1967, *J.Atmos.Terr. Phys.*, 35, #1, 153-163 (1773).

16.M.S. Gussenhoven, D.A.Hardy and N.Heinemann, Systematics of the equatorward diffuse auroral boundary, ***Cosmicheskie issledovaniya,*** in Russian, 88, #7, 5692-5708 (1983).

17.J.Oksman, Apparent diurnal movements of the trough in total electron content (TEC) of the ionosphere, ***Geophysica,*** 19, #1, 13-22 (1982).

18.Yu.I.Galperin, G.Cranye, Yu.V.Lisakov et al., Diffuse auroral zone. I. Model of the equatorial boundary of the diffuse zone of auroral electron precipitation for the evening and midnight, ***Cosmicheskie issledovaniya,*** (in Russian), 15, #3, 421-434 (1977).

19.M.G.Deminov, A.T.Karpachev, S.K.Annakuliev, V.V.Afonin and Ya. Smilauer, Dynamics of the ionization troughs in the night-time subauroral F-region during geomagnetic storms, *Adv. Space Res.*, in press (1995).